

PROCEEDINGS OF SPIE

[SPIDigitalLibrary.org/conference-proceedings-of-spie](https://spiedigitallibrary.org/conference-proceedings-of-spie)

Automated measurement of fetal right-myocardial performance index from pulsed wave Doppler spectrum

Rahul Suresh, Srinivasan Sivanandan, Nitin Singhal, JinYong Lee, Mi-Young Lee, et al.

Rahul Suresh, Srinivasan Sivanandan, Nitin Singhal, JinYong Lee, Mi-Young Lee, Hye-Sung Won, "Automated measurement of fetal right-myocardial performance index from pulsed wave Doppler spectrum," Proc. SPIE 10950, Medical Imaging 2019: Computer-Aided Diagnosis, 109500L (13 March 2019); doi: 10.1117/12.2512402

SPIE.

Event: SPIE Medical Imaging, 2019, San Diego, California, United States

Automated Measurement of Fetal Right-Myocardial Performance Index from Pulsed Wave Doppler Spectrum

Rahul Suresh, Srinivasan Sivanandan, Nitin Singhal^a, JinYong Lee^b, and Dr Mi-Young Lee, Dr Hye-Sung Won^c

^aSamsung R&D Institute - Bangalore, India

^bSamsung Medison - Pangyo, South Korea

^cDepartment of Obstetrics and Gynecology, University of Ulsan College of Medicine, Asan Medical Center, Seoul, Korea

ABSTRACT

Congenital heart disease is the leading cause of birth defect related deaths. The modified myocardial performance index of the right ventricle (R-MPI) is a sensitive and early clinical indicator of fetal cardiac health. Objective repeatable measurement of R-MPI is an important deciding factor for the clinical adaptation of the R-MPI. In this work, we describe a novel method for automatic computation of R-MPI from the Pulsed Wave Doppler (PWD) images. Our method involves a Fourier series based cardiac cycle detection followed by an adaptive windowed energy based valve click localization and weighted gradient based refinement. Using this method, we have been able to measure R-MPI reliably with a mean difference of 0.0075 ± 0.034 from 170 expert annotations on 68 fetal PWD images with an Intra-Class Correlation (ICC) of 0.9380. Furthermore, we have introduced novel methods for normalization and synchronization of PWD images acquired at two different time intervals for the assessment of iso-volume time intervals and an accurate measurement of R-MPI.

Keywords: Fetal Heart, Ultrasound, Doppler, Fetal Heart Rate, Myocardial Performance Index

1. INTRODUCTION

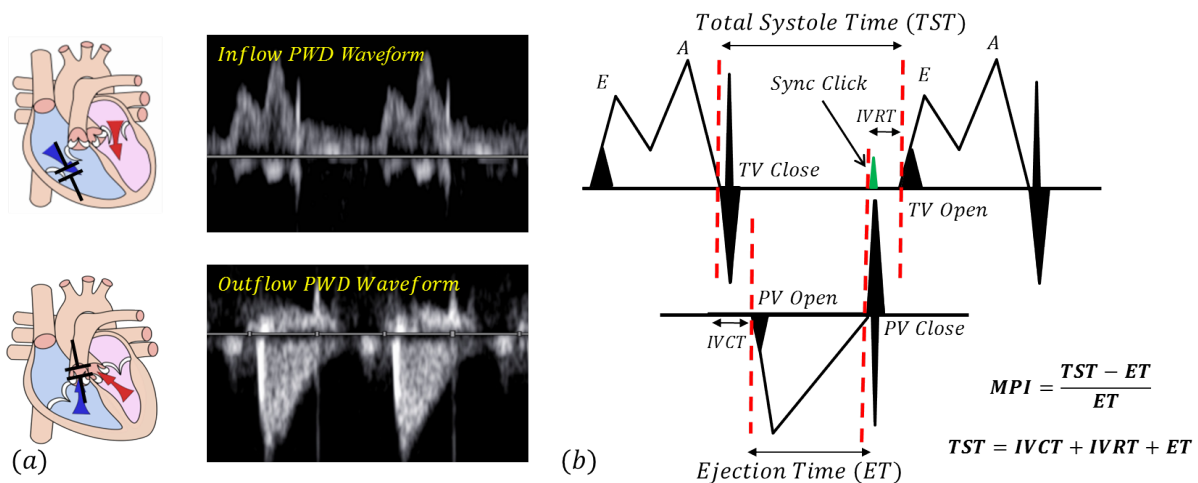


Figure 1. (a) Doppler gate placement for R-MPI measurement (Heart illustration courtesies of wikimedia commons^{1,2}) Caliper (red line) placement for R-MPI measurement. (color image)

The modified myocardial performance index or MPI has been found to be a sensitive indicator of fetal cardiac health in pathologies like Intra-Uterine Growth Retardation, Twin-to-Twin Transfusion Syndrome, Small-for-Gestational Age fetuses and Maternal Diabetes.³ The MPI is computed from the Iso-Volume Contraction Time (IVCT), Iso-Volume Relaxation Time (IVRT) and the Ejection Time (ET) (Fig. 1(b)). Since the fetal heart

is right-dominant, the R-MPI may prove to be an early indicator in the development of pathologies.⁴ Clinical measurements of MPI consist of manually placing caliper markers for measuring time intervals between valve click events in the PWD image (Fig. 1(b)). The fetal left MPI (L-MPI) is usually measured by identifying valve clicks in a single PWD image acquired at the junction of Mitral Valve and Aortic Valve. However, in the case of right side of the heart, the tricuspid valve (TV) and pulmonary valve (PV) are anatomically placed in such a way that it is not possible to acquire blood flow waveforms at TV and PV in the same doppler acquisition.⁴ In order to measure R-MPI using PWD, two separate images are acquired, one at TV (ventricular inflow) and another at PV (ventricular outflow) as shown in Fig. 1(a).

As MPI is a ratio of two time-intervals, it is very sensitive to the placement of the markers. Consequently, fetal MPI estimation requires a substantial learning curve to achieve competence.⁵ Due to this, there is large subjective variation in the normal ranges of the MPI values reported in clinical studies.⁴ Therefore, objective and repeatable measurement of MPI is an important first step for wider clinical adaptation of this bio-marker.⁶ Existing methods for automated measurement of MPI proposed in literature^{7,8} use the peak of valve click signals for estimating the time intervals. However, a recent study⁹ has shown the start of the valve click to be a better marker for measurement as shown in Fig. 1(b). Furthermore, all the existing methods for MPI estimation use many empirical parameters requiring fine tuning and validation.

R-MPI measured directly using absolute time intervals obtained from two separate PWD acquisitions are usually inaccurate as the fetal heart rate has a large beat-to-beat variation (5 to 15 beats per minute in normal cases¹⁰). This results in the inflow and outflow images typically having different heart rates (both intra- and inter-image). Furthermore, due to the lack of one-to-one correspondence between the inflow and outflow valve click events, there is no existing method to measure the iso-volume time intervals for the right side of the fetal heart.

In this paper, we propose a robust, non-empirical and generalizable approach for the measurement of R-MPI from PWD images. Section 2 describes a coarse-to-fine detection method for the accurate localization of cardiac cycle and valve clicks. Section 3 discusses the experimental results and the clinical validation.

2. METHODOLOGY

For a reliable estimation of R-MPI, it is necessary to detect the individual cardiac cycle (CC) and valve click (VC) positions separately and accurately. Our method involves (a) CC detection and (b) VC localization using a novel signal processing pipeline. This method (Fig. 2) consists of a novel “coarse-to-fine” strategy wherein we detect the coarse CC and VC range (inflow/outflow peaks) followed by refinements for accurate CC and VC positions. The CC and VC peak detections are difficult due to the presence of multiple peaks in the input signal which pose a challenge for an elementary peak detection algorithm. Therefore, as a first step, it is important to reliably detect a given peak in every heart cycle of the PWD image.

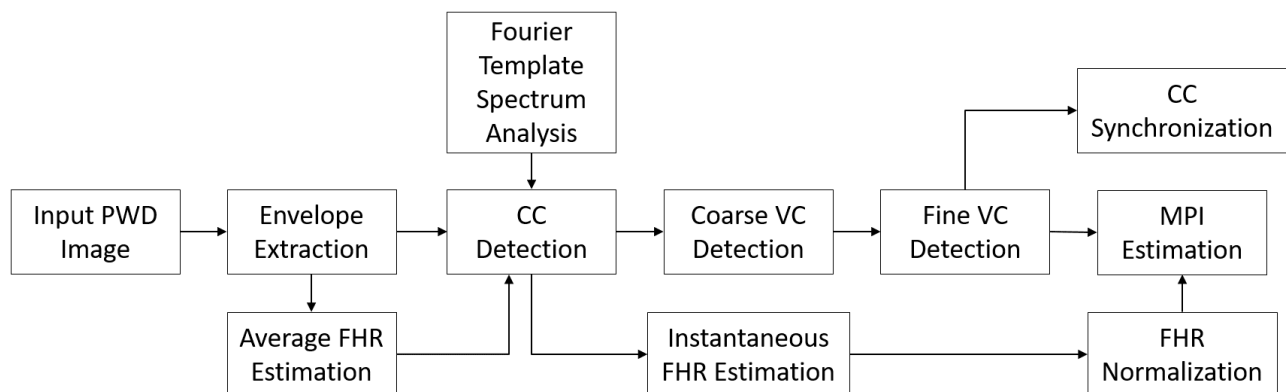


Figure 2. Flowchart of proposed method for automated estimation of R-MPI (FHR - Fetal Heart Rate).

2.1 Cardiac Cycle Detection

As a first step, we extract the envelope of the incoming signal using k-means ($k=2$) clustering¹¹ to distinguish between foreground and background pixels in the input PWD image. To detect the instantaneous cardiac cycle in the inflow/outflow waveforms, we must be able to reliably detect a feature point in the respective waveforms in every cycle. We choose to detect the “A” peak (Fig. 1(b)) in the inflow and the peak of the outflow signal respectively. As an elementary peak detection algorithm cannot differentiate between the flow peaks, valve click peaks and other spurious peaks, all peaks other than the peaks of interest act as *noise*.

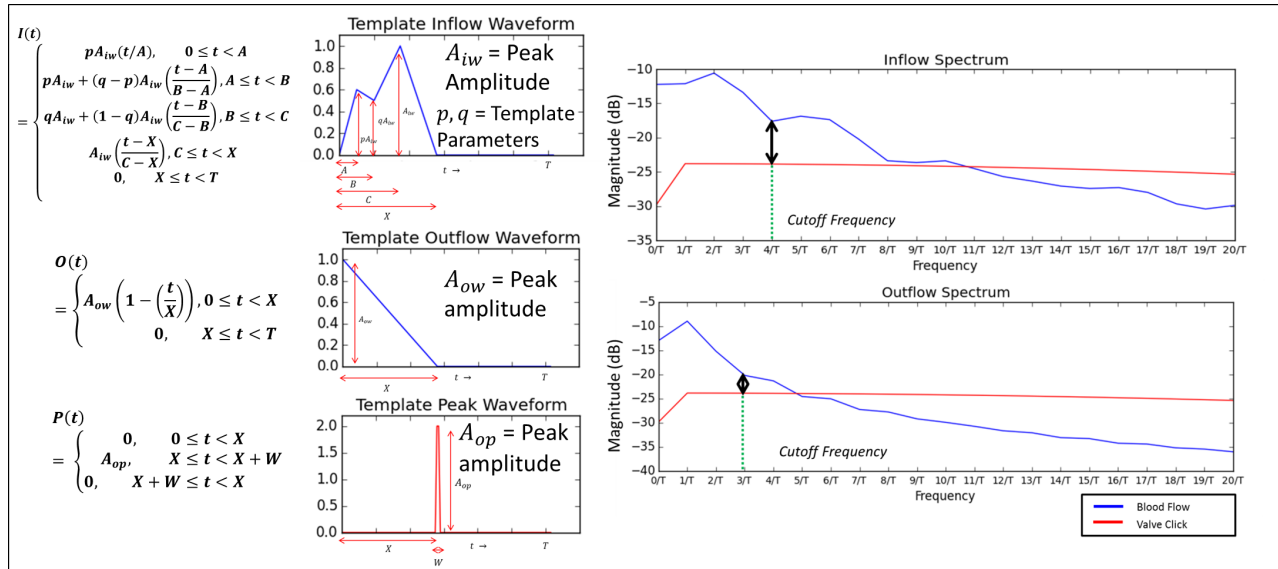


Figure 3. (a) Construction of template waveforms, (b) Magnitude spectrum of inflow and outflow waveforms in comparison with the valve click signal. (color image)

To aid in the process of discrimination, we perform a Fourier series analysis of a template inflow/outflow waveform and a template “peak” waveform (of the kind which are typically observed in the PWD image acquired from the right ventricle). The template waveforms are constructed in a time interval T and assumed to be repeating as shown in Fig. 3(a). Our purpose of constructing a template signal is to obtain a parameterized analytical representation of the general blood flow and valve click waveforms which could be used for discriminating them based on their harmonic composition. The fundamental frequency ($1/T$) for the harmonic decomposition is set using the *average heart rate*. The average heart rate is computed as the peak-amplitude frequency of the magnitude spectrum of the Fast Fourier transform of the input waveform. As can be observed in Fig. 3(b), the magnitude spectrum of the inflow/outflow waveforms and the “peak” waveforms “cross” at a particular harmonic of the fundamental frequency. We choose a harmonic frequency (parameterized by $T = \text{cardiac interval}$) where the SNR of the template waveforms is significantly higher (5dB) than the “peak” spectrum. This allows us to reject the peak waveform in the input signal and retain only the flow waveform. From Fig. 3(b), the cutoff harmonics (n) chosen are $n=4$ and $n=3$ for inflow and outflow waveforms respectively. By filtering the waveforms with this harmonic cutoff, we can *extract* or *reject* the peaks of interest. The Fourier analysis approach allows us to analyze an ideal waveform and extend the results to real-world signals. This representation of the cutoff frequencies in terms of harmonics helps us in designing filters that are robust and generalizable to a wide range of fetal heart rate.

With this analytical approach, we filter the envelope of the real world inflow/outflow waveforms using a low-pass filter with a cutoff of the first harmonic (first signal) and a cutoff of the n^{th} harmonic (second signal) as shown in Fig. 4. We detect peaks in the first signal and the second signal and retain those in the second signal which are closest to the first. This location of the peak serves as a coarse estimate of the actual peak in the original waveform. By searching in an appropriate neighborhood of this peak (Fig. 4) in the original envelope signal, we

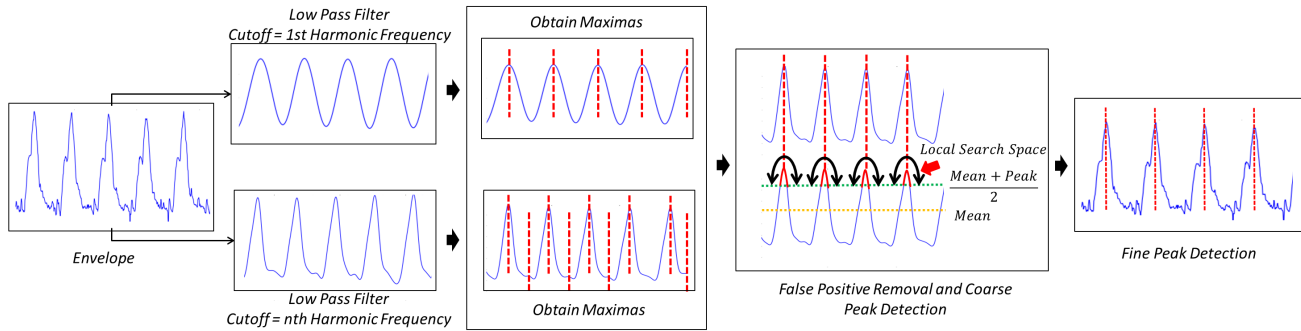


Figure 4. Cardiac cycle detection algorithm. (color image)

can determine the true peak location (“A” peak of inflow and the peak of outflow waveforms). Essentially, the results obtained from the Fourier analysis have been combined *non-linearly* to estimate the peak position.

2.2 Coarse Valve Click Detection

Our proposed method for valve click detection involves a coarse-to-fine approach. The windowed energy of the envelope is calculated as the energy of the signal in a window around a given time position. The energy is calculated with the window placed at every position in the envelope signal as shown in Fig. 6(a). By choosing the window size as the approximate width of the blood flow waveforms, we can obtain the window boundary with maximum energy. This boundary represents the approximate location in which most of the energy lies. Thereby, this also represents the coarse location of the valve clicks from the fact that there is a valve click event before and after every blood flow waveform (Fig. 1(b)).

The efficacy of the coarse localization step crucially depends on choosing a window size which is approximately correct. The window sizes can be computed by dynamic time warping a template inflow/outflow signal with the input envelope signal in a given cardiac cycle. For the purpose of matching, the template of Fig. 3(a) is parameterized with A_{iw} as the amplitude at blood flow peak and X as $0.5 * \text{cardiac cycle width}$ (Fig. 5). The warping path is obtained as the minimum cost path traced on the matrix computed using cost function Eq. 1.

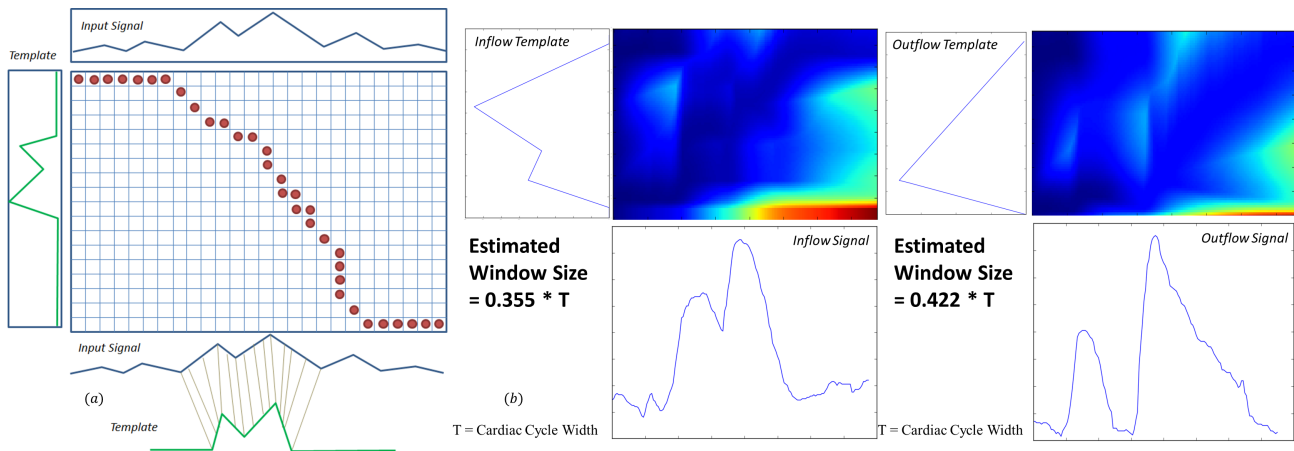


Figure 5. (a) Dynamic time warping method, (b,c) Example of window size estimation for inflow and outflow respectively. (color image)

$$Cost(i, j) = |S(i) - T(j)| + \min \begin{cases} Cost(i-1, j-1) \\ Cost(i, j-1) \\ Cost(i-1, j) \end{cases} \quad (1)$$

In Eq. 1, $S(i)$ represents the envelope signal amplitude at sample i , $T(j)$ is the template signal amplitude at sample j and $Cost(i, j)$ represents the cost computed for match between signal value at location i and template value at location j . By warping the input envelope signal w.r.t the template signal, we can compute the window size (width of the blood flow waveform) from Eq. 2.

$$WindowSize = X * (InputSignalLength/WarpedSignalLength) \tag{2}$$

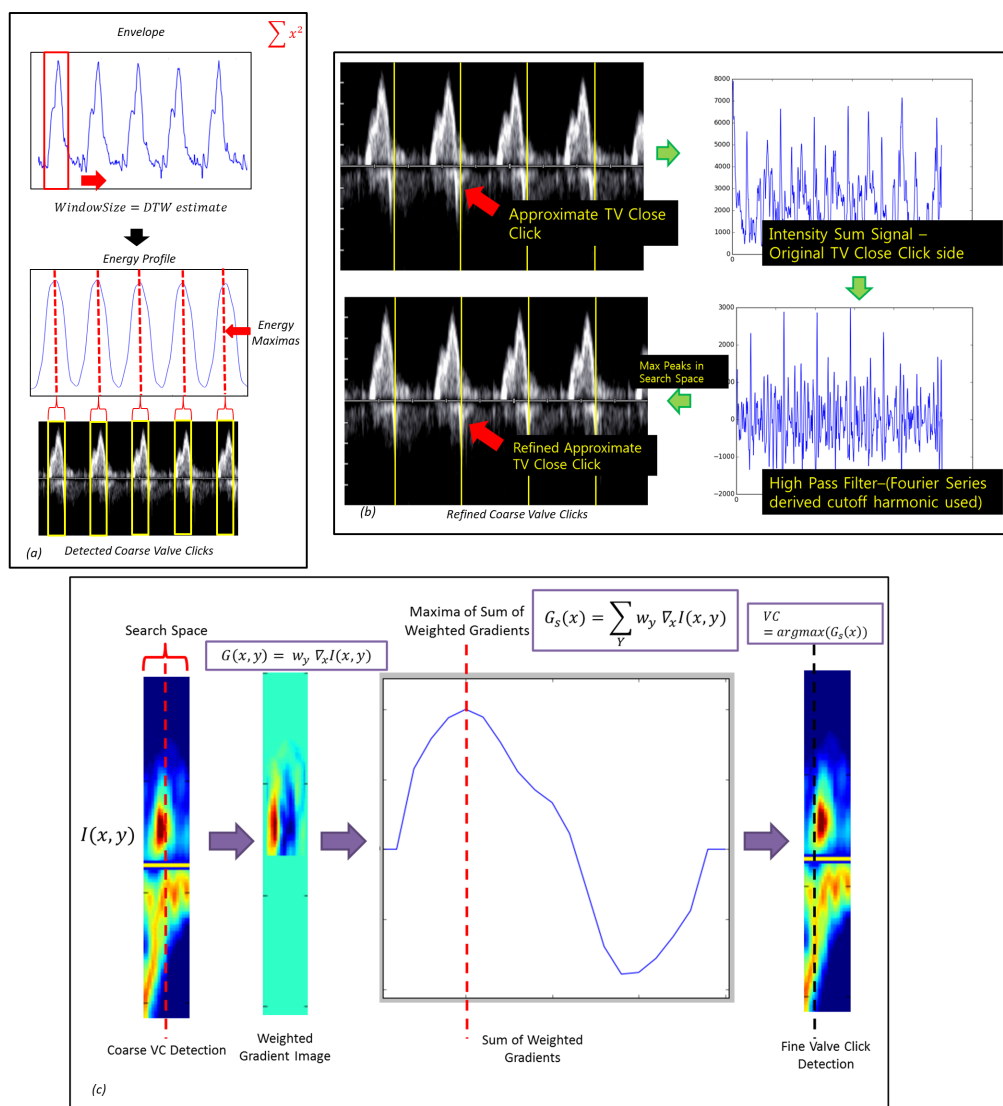


Figure 6. (a) Coarse valve click detection, (b) Coarse valve click refinement, (c) Fine valve click detection. (color image)

The detected coarse locations of TV and PV open VCs are very close to the actual VC location. To further improve the coarse detection of TV close and PV close VCs, we use an intensity sum signal derived by adding up all the intensity values for a given time position. We use a high pass filter on this signal to detect the VC peaks. The cutoff frequency for this filter is the same as the one used in the low-pass filter for the CC detection.

In a search space around the windowed coarse VC detection, we search for the maximum in the high pass filter output. This location is our improvement of coarse detection of the TV close and PV close locations. Using the same harmonic cutoff (as in the CC detection) allows us to extract the VC peaks and reject the surrounding high frequency noise (Fig. 6(b)).

2.3 Fine Valve Click Detection

To detect the VC positions accurately, the temporal gradient map $G(x, y)$ of the intensity values $I(x, y)$ of inflow and outflow images are calculated in a search space around the approximate VC positions (here x represents the horizontal time axis and y represents the vertical velocity axis in the PWD image). A weighted gradient sum $G_s(x)$ is calculated at each position in the search space around the coarse VC position, where the weights w_y are a function of the intensity of the pixel and y -distance (vertical distance) from reference line of the PWD image (as shown in Fig. 6(c)) (Eq. 3). The weight function is calculated using Eq. 4 where $\alpha \in (0, 1]$ is a tuning parameter. This is chosen so as to favor a high gradient closer to the reference line. The positions of the maxima of the weighted gradient sum are the final VC positions.

$$G_s(x) = \sum_{\forall y} w_y \nabla_x I(x, y) \quad (3)$$

$$w_y(x, y) = \alpha^y I(x + 1, y) \quad (4)$$

2.4 Heart Rate Normalization

The fetal heart rate has a large beat-to-beat variation (5 to 15 beats per minute in normal cases).¹⁰ As the PWD signals at TV and PV are acquired at two different time intervals, the ventricular inflow and outflow images would typically have different heart rates (both intra- and inter-image). Hence, for the accurate computation of MPI values, it is necessary for both the cardiac cycles in consideration to be analyzed in the same time *scale*. Consequently, we normalize the two images by either stretching or compressing them by the ratio of the heart rates of the two cycles under consideration. This calibrates all the time scales so that an accurate MPI value can be computed. The instantaneous heart rates are computed from the CC detection algorithm (section 2.1).

2.5 Inflow/Outflow Synchronization

As the ventricular inflow and outflow signals are acquired at two separate time intervals, there is no direct method for the measurement of iso-volumic time intervals (IVCT and IVRT). In order to calculate IVCT and IVRT, we identified a key-point in inflow image which corresponds to the same event in outflow image. Among all the fetal PWD images obtained for evaluation, we observed a consistent low amplitude signal in the inflow image (sync click as shown in Fig. 1(b)) which corresponds to the PV close signal in the outflow image. Using this signal, we were able to synchronize the inflow and outflow images to obtain the IVCT and IVRT intervals. The detection of the sync click event followed a similar algorithm to the one described for the valve click events (section 2.2, section 2.3).

3. EXPERIMENTAL RESULTS AND DISCUSSION

3.1 Dataset and Clinical Reference Acquisition

All the datasets used for the analysis were acquired using a C2-6 curvilinear probe on Samsung Medison WS80A ultrasound equipment in accordance with the guidelines established by the Institutional Review Board. The start of the opening, closing and synchronization valve clicks were annotated by an expert (using an in-house developed annotation tool) and were used as clinical reference for our experiments.

Valve Click	Total Annotations	Detections within $\pm 5ms$	Detection Rate
TV Open	199	196	98.49%
TV Close	179	166	92.74%
PV Open	200	194	97.00%
PV Close	200	192	96.00%
Sync Click	195	186	95.38%

Table 1. Detection results using our algorithm

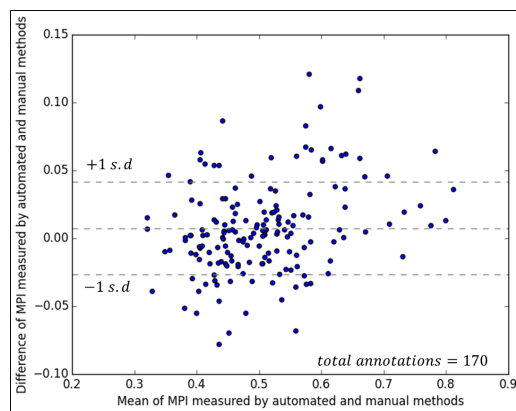


Figure 7. Bland-Altman plot for the measured R-MPI values indicating the accuracy of our detections in comparison to clinical reference. (**color image**)

3.2 Quantitative Results

We have evaluated our VC detection algorithm on 68 fetal PWD image datasets (with 2-3 cardiac cycle annotations per image) using valve clicks annotated by a clinical expert. The detection rates were calculated as the ratio of detections within $\pm 5ms$ and the total number of valve click annotations. Using this method, we have achieved detection rates for the valve clicks within $\pm 5ms$ from annotations as shown in Table 1. The MPI values were compared on 170 annotations where all 4 valve clicks and sync click were marked by the expert. Using our method, we have achieved a mean difference \pm standard deviation of 0.0075 ± 0.034 from expert annotations (Fig. 7). The intra-class correlation (ICC) between MPI values calculated using the automated solution and expert annotations was obtained as 0.9380. The above quantitative results show the robustness of our method in measuring R-MPI at par with clinical expert opinion. Fig. 8 shows representative results of our algorithm with quantitative measurements obtained after normalization and synchronization of the input images.

3.3 Discussion

The analytical Fourier series approach generalizes well to real data. The filter cutoffs parameterized as harmonics enables our algorithm to perform robust cardiac cycle and valve click detection even in the presence of large variations in fetal heart rate. Further, the dynamic time warping based window size estimation ensures that the blood flow waveform width and (thereby) the coarse localizations of valve clicks are detected even in case of pathological conditions where the blood flow intervals are smaller in comparison to the total cardiac cycle. To support this claim, we generated synthetic inflow datasets with blood flow intervals as varying ratios [0.1-0.5] of cardiac cycle width. Table 2 shows the comparison of actual ratios used for generating the synthetic data with the estimated window size (computed by dynamic time warping) as ratio of cardiac cycle.

4. CONCLUSION

In this work, we have described a novel Fourier analysis based approach for the computation of R-MPI. Unlike existing methods for MPI measurement, our analytical approach enables us to design an algorithm without using empirical low-pass filter cutoffs and heuristic complex composite equations. This makes our method easily generalizable and extensible to a wide range of fetal heart rate and pathologies observed in the case of R-MPI measurement.

List of Abbreviations

PWD: Pulsed Wave Doppler	CC: Cardiac Cycle	VC: Valve Click
TST: Total Systole Time	ET: Ejection Time	IVCT: Iso-Volumic Contraction Time
IVRT: Iso-Volumic Relaxation Time	TV: Tricuspid Valve	PV: Pulmonary Valve

Actual Blood Flow Width	Estimated Window Size
0.1	0.1217
0.2	0.2115
0.3	0.3012
0.4	0.4038
0.5	0.5

Table 2. Actual blood flow width and estimated window sizes as ratios of cardiac cycle width

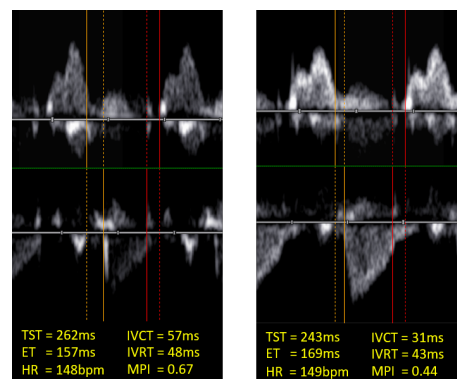


Figure 8. Results of our method with measurement values after normalization and synchronization. (color image)

REFERENCES

- [1] Wapcaplet, Reytan, and Mtcv. <https://commons.wikimedia.org/w/index.php?curid=4158464>.
- [2] Wapcaplet. <https://commons.wikimedia.org/w/index.php?curid=67876>.
- [3] Lee, M.-Y. et al., "Fetal left modified myocardial performance index measured by the auto mod-mpi system: development of reference values and application to recipients of twin-to-twin transfusion syndrome," *Prenat. Diagn.* **36**(5), 424–431 (2016). PD-15-0647.R1.
- [4] Maheshwari, P. et al., "The fetal modified myocardial performance index: Is automation the future?," *Biomed Res Int.* **2015** (2015).
- [5] Cruz-Martinez, R. et al., "Learning curve for doppler measurement of fetal modified myocardial performance index," *Ultrasound Obstet Gynecol* **37**(2), 158–162 (2011).
- [6] Avnet, H. et al., "Automation of the fetal right myocardial performance index (rmpi) to optimise repeatability," *Ultrasound Obstet Gynecol* **50**, 170–170 (2017).
- [7] Wang, J. et al., "Automated cardiac time interval measurement for modified myocardial performance index calculation of right ventricle," *IEEE EMBC*, 7288–7291 (Aug 2015).
- [8] Yoon, H. et al., "Automated measurement of fetal myocardial performance index in ultrasound doppler waveforms," *Proc. SPIE* **9040**(1), 9040–9040 (2014).
- [9] Lee, M.-Y. et al., "Feasibility of using auto mod-mpi system, a novel technique for automated measurement of fetal modified myocardial performance index," *Ultrasound Obstet Gynecol* **43**(6), 640–645 (2014).
- [10] Hornberger, L. K. et al., "Rhythm abnormalities of the fetus," *Heart* **93**(10), 1294–1300 (2007).
- [11] Hartigan, J. A. and Wong, M. A., "Algorithm as 136: A k-means clustering algorithm," *J R Stat Soc Ser C Appl Stat* **28**(1), 100–108 (1979).